RESEARCH ARTICLE **ISSN 2738-9898 (Print) ISSN 2738-9901 (Online)**

Floodplain mapping of an ungauged river: A case study on Seti River in Pokhara, Nepal

Keshav Basnet[1*], Deepak Acharya[1], Krishna Prasad Bhandari[1], Suraj Lamichhane[2], Biwas Babu Sadadev[1]

[1]Department of Civil Engineering, Pashchimanchal Campus, Institute of Engineering, Tribhuvan University, Nepal

[2]Department of Civil Engineering, Pulchowk Campus, Institute of Engineering, Tribhuvan University, Nepal

* Author to whom correspondence should be addressed; E-Mail: basnet.keshav@gmail.com

Received : 5 September 2023; Received in revised form : 21 September 2023; Accepted : 26 September 2023;Published: 25 January,2024

Abstract

Settlements and infrastructures along the banks of Seti River in Pokhara, Nepal are at high risk of flood. Floodplain mapping for ungauged Seti River is not straightforward like the one for gauged rivers. Main goal of this study was to prepare floodplain maps along the ungauged Seti River in Pokhara, as a case study, using one-dimensional HEC-RAS model. First, catchment area ratio (CAR) method was applied to find annual flow in ungauged Seti River based on flow data of gauged Mardi station. Once the annual maximum flow was estimated for sufficient time length (i.e., 42 years), peak flood was predicted using Gumbel method for various reaches of Seti River within Pokhara. Thus, estimated peak floods were also compared with the peak floods predicted using Gumbel method based on the annual flow data of Tanahu station. As the specific discharge observed to be comparable with each other (difference ≤ 2.68%), CAR method found be a reliable one that is useful for ungauged river. Then, Cowan's approach was applied to estimate Manning's roughness coefficient (n) and used it for calibration of HEC-RAS model. Cowan approach found to be a best alternative for ungauged river as the comparison of modelled flow depth with measured flow depth yielded only 3.82% difference. Finally, 1D hydraulic modelling was performed using calibrated HEC-RAS model with available 12.5 m resolution DEM terrain data. Floodplain maps were prepared based on the HEC-RAS simulation results coupled with Google Earth map. The flood inundation area within Pokhara was found to be 2.76, 3.05, and 3.59 Km^2 for the peak flood of 20, 50, and 100 years return periods, respectively. Moreover, Laltin Bazar and Gaighat areas were identified to be at high risk of flood such that these areas found to be inundated with 20 or greater years return period floods, compared to Ramghat area which was observed to be flooded with the peak flood of 50 or more years return period. Floodplain maps of this study could be used for preparing flood hazard maps, planning infrastructures, and flood management.

Keywords: Catchment area ratio method, Cowan approach, Flood management, HEC-RAS, Inundation, Manning's roughness coefficient

1. INTRODUCTION

The total length of rivers in Nepal is 45000 km from 6000 rivers, with the drainage density of 0.3 per Km^2 [1]. River analysis is important for infrastructure planning and development. Further, hydraulic analysis of a river flow is necessary to be performing for planning and designing of hydraulic structures at the river [2]. Nepal is in the first 30^{th} country that is at the risk of flood and landslide. So, national planning strategies have been developed for risk reduction of the floods and landslides in GIS base technologies and to tie up with the universities and academic institutions [3]. Pokhara is the major city of Kaski district, which lies in the central part of Nepal as shown in Fig. 1c. Pokhara, the second largest city in Nepal, offers a wide variety of interests (lakes, caves, gorges, and scenic glaciated mountains) related to its catastrophic geomorphologic evolution [4]. Seti River passes through this beautiful city [5]. About 4,700m of river flows through the deep cutting gorges within the city, and the remaining about 30,000m of river flows down the bank of the city. Also, this river is the nearest source of construction materials like sand and aggregate for the city. Multiple hazards and risks are rapidly increasing in Pokhara due to unsustainable land use practices, particularly the increase in built-up areas. Pokhara, being the capital of Gandaki Province, urbanization in this area is expanding. According to the prediction analysis, by 2030 A.D., about 25% of the urban/built-up area will be increased in risk zone of different hazard, among this, about 6.2% of urban/build-up area will be in special attention zone, which will be in risk of different type of hazards of flood, landslide, sinkhole, and edge fall [6]. Proper planning and management are an essence up to our planning horizon. For all these reasons, we focused our investigation in Pokhara and selected the corresponding catchment area that lies in the middle part of the Kaski district, as illustrated in Fig. 1a, as our study area. Catchment area of interest along the Seti River with 12.5m resolution DEM is presented in Fig. 1b. During the monsoon, the flow through the gorges of Seti River will have insufficient water way, so the pounding effect occurs, which causes flood. Imprudent habitation in lowest terrace and floodplain of Seti River is found in study area [8]. Floodplain map of the Seti River deems necessary for pre-planning the disaster, planning the infrastructures, development of industrial, agricultural, and touristic facilities projects, including re-creational projects, around the riverbank in the city. Also, this map could be helpful in controlling water pollution and making plans for solid waste management. However, floodplain map preparation by developing a reliable model with a comparable value of parameters is an essence. The model output may not be the same for a model with the same parameter [9]. The number of bridges, hydro-power plants, headwork for irrigation projects, dense settlements, agricultural lands, and construction materials quarry areas around the bank of the river have been noted throughout the channel length along the Seti River. Similarly, settlement around the study area is also in risk of flood. For example, flooding occurs in Ramghat area of Pokhara, every year. An example of flooding event in the Ramghat location, which lies in our study area, is shown in Fig. 2. The flood occurred during 5^{th} May 2012 was measured about 397.9 m^3/s by the Irrigation Development Office, Kaski was devastating one in this area. The road was washed in the bending bank of Seti River. Therefore, expanding settlement density along the bank of the Seti River will be affected, if not managed properly on time.

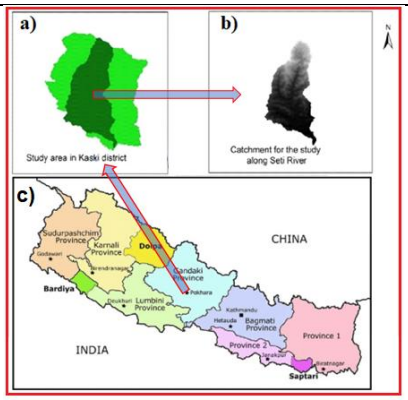

Figure 1: Study area: a) Kaski district with study area (represented by dark green colour); b) Catchment area of interest (i.e., study area) with 12.5m resolution DEM; c) Map of Nepal showing the location of Pokhara City (where our study was focused), capitol of Gandaki Province that lies in the central part of Nepal. New map of Nepal was taken as a reference from [7].

Figure 2: An image showing a flood example at Ramghat that lies in the study area (Source: Bhupal Creation, YouTube)

Floodplain is the land area that is susceptible of being inundated by water from any source of water. It is a tool to understand the risk of flood along the water body. Hydraulic analysis is necessary for analysis of flooding source carried out to provide estimates of the elevations of floods of selected recurrence intervals. Floodplain mapping using a calibrated hydraulic model might be an alternative. Computer aided process engineering modelling is increasing in recent years towards advanced modelling tools [10]. Flood forecasting and inundation mapping have been developed in the past with rapid advancement in computer technology and research in numerical techniques with various one-dimensional hydro-dynamic models [11]. The cross-cutting issues like climate change, disaster risk management etc. are the motivation for the flood hazard mapping. The floodplain mapping has been made extensively in the GIS environment. Hydrologic analysis of a flooding source carried out to establish peak flood discharges and their frequencies of occurrence. These two analyses are necessary for knowing the flood level during a flooding event. This can be performed with modelling software like HEC-RAS and MIKE Flood [12]. Access to MIKE Flood is difficult as it is commercial software. We used a freely available and widely used HEC-RAS model [13].

HEC-RAS had been used extensively from 1964 AD, developed by American Army Corps of Engineers for hydraulic modelling of River, which consists of some useful graphical user interface for easy analysis, visualization, and interpretation of results. The floodplain maps have been prepared by analysing river with HEC-RAS throughout the world (e.g., [14], [15], [16], [17], [18]). [11] performed a study with calibration of HEC-RAS to predict flood in lower Tapi River, India. [17] used HEC-RAS to develop floodplain maps for the part of Kabul River in Pakistan. Further, [19] conducted research on the flood risk mapping in east

Rapti River using HEC-RAS and GIS. They suggested that the GIS supports as an excellent tool for flood risk mapping like in this study. [20] used HEC-RAS to prepare flood hazard mapping of Bagmati River in Kathmandu valley of Nepal. However, the 30m resolution DEM data they used was not sufficient for the analysis of such hazard mapping. [15] studied the flood hazard map in Rupandehi district. However, they used the approximated value of Manning's roughness coefficient (n). [21] tried for flood hazard mapping of Bishmumati River, in Kathmandu. Again, their study was limited to the use of 30m resolution DEM data and the use of approximated "n" value. Therefore, though, there are few research efforts have been made in the rivers of Nepal for hydraulic modelling using HEC-RAS (e.g., [18], [22]), they lack the calibration of the model. As HEC-RAS has not been used yet extensively in Nepal, its proven reliability might support it's used on the rivers of Nepal. So, it is important to calibrate the model before using it for floodplain mapping. Roughness coefficient being a critical parameter in the gravel bed river [23], the reliability of its value defined the accuracy of the prepared floodplain maps for the rivers in Nepal. Therefore, we calibrated the HEC-RAS model before using it for simulation to prepare floodplain map based on the parameter - Manning's roughness coefficient. [6] tried for the multi hazard risk map of Pokhara; still there was not any hydraulic analysis of the river for flood prediction. [24] performed a hydraulic modelling study using HEC-RAS, but their study focused only in Ramghat area of Pokhara. [18] initiated a study, though incomplete, of flood hazard mapping for Seti River and provided some preliminary results in the Lecture Notes in Civil Engineering. The main objective of this study was to prepare the floodplain map of ungauged Seti River, within Pokhara Metropolitan City using calibrated HEC-RAS model. First, the annual maximum flow of the ungauged Seti River was estimated using catchment area ratio method based on the gauged flow data of Mardi station. Then, the peak flood for the study area with 20, 50, 100 years return period was predicted using Gumbel method. The calibrated HEC-RAS model with Manning's roughness coefficient (n), estimated using Cowan approach, was used for the simulation of Seti River flow. Finally, the floodplain maps for Seti River in Pokhara was prepared for the three return periods based on the results of 1D HEC-RAS modelling coupled with Google Earth Map.

2. METHODOLOGY

2.1 Selection of Study Area

Kaski is a district of Nepal with high intensity of rainfall throughout the year [1]. The study area falls in this district, which lies in the central part of Nepal, as shown in Fig. 1. The study area lies in between 28°05'30.84" to 28°35'24.09" North and 83°49'1.98" to 84°04'46.10" East. The catchment area (i.e., study area) is about 535 km^2 with its elevation ranging from 7000m to 500m amsl. Annual mean monsoon precipitation ranges from 1600mm to 4500mm in the catchment area [25]. This catchment contains various types of land use: agricultural land, dense forest, farmland, steep slopes etc. Seti River, which flows in deep gorges through the central part of Pokhara City, floods during the monsoon in different flanged part of the river causes side cuttings and inundation of settlements [24]. Similarly, there is large side-bank erosion through its channel length in Kaski. According to [8], imprudent human settlement in the lowest terrace and floodplain of Seti River is found in the Pokhara City (e.g., Fig. 2). Seti River analysis in Pokhara could be significant for the proper planning and development of infrastructures within the vicinity of the river. For the study of Seti River flooding, we were focused within the Pokhara Metropolitan City that covers about 34 Km (Fig. 3). In Fig. 3, number along the river represents the ending/starting location of a reach. The river was discretized into 11 reaches total for modelling purpose.

Figure 3: Area of interest for floodplain mapping along the Seti River, represented by white line, within the Pokhara Metropolitan City

2.2 Catchment area calculation

Catchment area and precipitation are the major variables that determine the surface runoff. Catchment area is essential for peak flood calculation from empirical formula. Catchment area was calculated using both the Google Earth Map and GIS with 12.5m resolution DEM as shown in Fig. 4 and found to be very close to each other. Total catchment area of 533.5 Km^2 (GIS result) with snow covered area of 53.8 Km^2 was used for peak flood calculation.

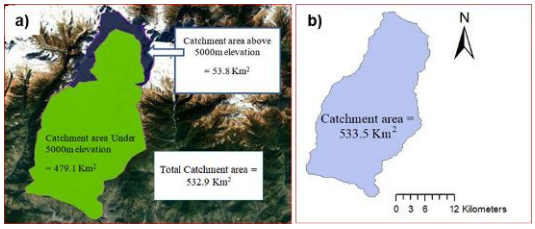

Figure 4: Catchment area calculation: a) Using Google Earth map; b) Using GIS with 12.5m resolution DEM.

2.3 Available in-situ discharge data

Previously surveyed data of the Water Resource and Irrigation Development Office, Kaski ensures that the slope of the river is less than 10% in the study section which is favourable for the use of HEC-RAS modelling. The flow and water depth data at the 80m long weir of headwork located at Tulsighat (Fig. 5) has been recorded by the Pokhara Water Conservancy and Irrigation Project, Pokhara. The peak flood over the weir for the consecutive 7 years is presented in Table 1. 11.0m^3/s water flow was assumed to be extracted from the total river discharge by irrigation project through the gate adjoining with the weir as shown in Fig. 5. As we observed in Table 1, there is significant variation in the recorded annual peak discharge though it has the same value for corresponding 3 years out of the measured data of 7 years. This peak discharge data, though limited, was used for preliminary simulations for calibrating the HEC-RAS model based on the parameter – Manning's roughness coefficient (n). The river in a short section has been analysed in HEC-RAS to find out the depth of the flow at very near the crest level of the weir

toward upstream side of river. The observed flow depth has been compared to the modelled flow depth for known discharge to calibrate the HEC-RAS model with varying values of Manning's n.

Figure 5: An image showing an example flow over the weir at Tulsighat

Table 1: Discharge data along with corresponding head measured by Pokhara Water Conservancy and Irrigation Project.

Measurement date of maximum yearly discharge	Head over the weir (m)	Maximum weir discharge (m^3/s)
7-Oct-09	1.5	251.3
30-31-Jul-2010	1.65	289.9
28-Jun-11	1.5	251.3
5-May-12	2	386.9
15-19-Jun-2013	1.25	191.1
18-Jul-14	1.5	251.3
29-Jul-15	1.35	214.5

2.4 Hydrological analysis

2.4.1 Catchment area ratio (CAR) method

We considered the Seti River flowing through Pokhara City as ungauged river because the annual measured flow data was limited for short period (i.e., 7 years). On the other hand, there was not any already developed stage discharge relation for our study area. The catchment area ratio (CAR) method is a potential alternative to estimate flood in ungauged river with reference to a gauged river [26]. Runoff, being the function of catchment area, this method can be used in estimation of flood for ungauged location with some modification if needed, supported by statistical analysis [27]. Mardi River, a tributary of Seti River, is assessed with the stream flow measurement gauge, having the catchment area of 160 Km^2 on the upstream side of Pokhara. Flow data from Mardi hydrological gauged station (DHM station no. 428) for 42 years was used as a basis while adopting CAR method to estimate the annual discharge of the ungauged Seti River. The relation between gauged and ungauged stations that exists in the CAR method is represented by the following equation [28]:

$$Q_{ungauged} = Q_{gauged} \times \frac{CA_{ungaged}}{CA_{gauged}} \quad (1)$$

where, $Q_{ungauged}$ = flood in ungauged station; Q_{gauged} = flood in gauged station; $CA_{ungagged}$ = Catchment area of ungauged station; CA_{gagged} = Catchment area of gauged station

2.4.2 Flood frequency analysis using Gumbel method

Once the annual maximum flow for the Seti River was estimated using catchment area ratio method, peak flood for different return periods was predicted using Gumbel method. Gumbel defined the Gumbel's distribution for extreme values. In hydrological study, peak flood was defined the largest flood of one year. The number of years is the sample number, should be in continuous basis [27]. The peak flood for three return periods (20, 50, and 100 years) was estimated using the Gumbel method with the equation for flood analysis as:

$$x_t = x_{mean} + K\sigma_{n-1} \quad (2)$$

where, x_t = value of variate x in occurrence interval t; x_{mean} = sample mean; σ_{n-1} = standard deviation of the sample size n; K = frequency factor. The predicted peak floods for Seti River, based on the data of Mardi station, are presented in Table 2.

Table 2. Comparison of predicted peak flood using Gumbel method based on the gauged data of Mardi station and Tanahu station.

	Peak flood using Gumbel method (m^3/s)		Peak flood per Km^2 (m^3/s per Km^2)		
Return period (years)	Based on data derived from CAR method with Mardi station data (catchment area = 160 Km^2)	Based on Tanahu station data (catchment area = 1505 Km^2)	Using CAR method based on Mardi station data	Based on Tanahu station data	Difference (%)
20	304.39	2860.85	1.9	1.9	0%
50	369.37	3537.32	2.31	2.35	1.70%
100	418.07	4044.24	2.61	2.68	2.68%

2.4.3 Verification of catchment area ratio (CAR) method

A peak flood per Km^2 for Seti River was calculated based on the peak floods predicted as described in section 2.4.1. In the same way, the corresponding peak floods were predicted using Gumbel method based on the available 16 years data of Tanahu station (DHM station no. 430.5), through which the Seti River drains off.

The estimated peak flood based on CAR method using Mardi station data found to be comparable with the peak flood based on Tanahu station data as presented in Table 2 resulting only 2.68% discrepancy in maximum.

This observation improved our confidence on the use of CAR method for ungauged Seti River as the Tanahu station data is limited (i.e., 16 years only) which could not be sufficient for long term flood analysis [27].

2.5 Estimation of Manning's roughness coefficient using Cowan approach

For the process of setting up a hydraulic model in the HEC-RAS, the geometric data, flow data, downstream reach lengths, resistant coefficient, energy loss, river confluence, and bifurcation are important [29]. When calculating the discharge with the Manning's formula, Manning's roughness coefficient is an important factor such that it is required to be determining precisely to validate the model. We calibrated the HEC-RAS model based on the roughness coefficient (Manning's n-value).

Cowan approach [30] was used to estimate this roughness coefficient value. Cowan breaks the Manning's value in six different factors: sediment size (n_o); degree of surface irregularity (n_1); variation of channel cross-section (n_2); effect of obstruction (n_3); vegetation (n_4); and degree of meandering (m_5). The total roughness (n) can be calculated from the following equation:

$$n = (n_0 + n_1 + n_2 + n_3 + n_4).m_5 \quad (3)$$

As suggested by Cowan all six roughness factors can be determined by visual observation and require no field measurements, although, n_0 may be estimated from other studies which relate roughness to sediment size and flow depth [31]. The base for the estimation of the Manning's roughness coefficient by the Cowan approach is provided in the Annex (Table A1) including components of the approach, their range within the river reach. Table 3 illustrates that the estimated value of Manning's roughness coefficient using the Cowan approach is 0.033 for the river section at Tulsighat near the weir, as an example.

Table 2: Estimation of the Manning's roughness coefficient for a river section at Tulsighat

Manning's component	Description of study river reach	Value
n_0	Dominantly coarse gravel	0.028
n_1	Minor degree of irregularity	0.005
n_2	Gradual	0
n_3	Negligible	0
n_4	No vegetation cover	0
m_5	Minor degree of meandering	1
Manning's roughness coefficient (n)	0.033	

2.6 Calibration of model with preliminary HEC-RAS simulations

Topographic data was converted into DEM to be used in HEC-RAS. The river centreline, riverbank, and flow path were defined following the cross-sections in random interval as suggested by the HEC-RAS 5.0 manual. Calibration of the HEC-RAS model used in this study was performed based on the single parameter, which is Manning's roughness coefficient (n), like in some other previous studies but outside of Nepal (e.g., [32]). This coefficient was estimated as per the Cowan approach as described in section 2.5. This account for the different geomorphologic, riverbed material's characteristics, and irregularity of the cross-section shape [31]. Some preliminary HEC-RAS modelling was performed for calibration purpose with varying values of Manning's roughness coefficient including estimated Manning's n based on Cowan approach for five different measured peak floods along with corresponding flow depths from Table 1. As illustrated in Table 4, the statistical analysis was performed with Nash-Sutcliffe efficiency, which was used for the prediction of the model efficiency in many hydrological studies, using the observed and modelled values of flow depth. The modelled flow depth using "n" value estimated based

on Cowan approach found to be only 3.82% different from the measured flow depth with the Nash-Sutcliffe efficiency of 0.951. Therefore, the Cowan approach found to be a reliable alternative for the estimation of Manning's roughness coefficient in the ungauged river. Overbank sectional variation of the Manning's roughness coefficient was not compared as the flow during the measured flood was observed within the normal riverbed section. As the roughness coefficient value of 0.0333 resulted from Cowan approach yielded the comparable flow depth from the preliminary HEC-RAS simulation (Table 4), it was taken for the further analysis. Not only this, but the Cowan approach was then applied for the

estimation of the "n" value for other reaches of the river where the discharge and flow depth data were not available.

2.7 Development of floodplain maps

First, the Seti River within the Pokhara Metropolitan City with 34.44 km length was segmented into eleven different reaches (Fig. 3) which have different catchment areas in their inlet node based on the condition of river channel, riverbed materials, junction of major tributary, meandering characteristics, riverbank conditions etc. Then, the input parameters for HEC-RAS were analysed for every reach. ALOS PALSAR DEM data was available in Alaska Satellite Facility. As shown in Fig. 1b, 12.5m resolution terrain corrected DEM data was used to calculate the catchment area of different required outlets into Seti River. The floodplain analysis of the river which flow through the narrow gorges is very difficult as topographic data doesn't represent such type of gorges where some modification required in the regular cross-sections extracted from the terrain model developed from DEM [33]. Out of eleven reaches, three reaches (reach 3, 5, and 7) were for deep gorges, where analysis of geographical characteristics from the available DEM was not successful as this DEM doesn't represent the river valley in these reaches. So, these reaches were not analysed in the post processing phase of the study. The specific peak floods for various reaches were calculated for 20, 50, and 100 years return period. Similarly, Manning's roughness coefficient for those reaches was estimated using Cowan approach.

Table 5 shows the value of the basic variables used in this study, including peak floods and Manning's n, for all the 11 reaches. These values of peak floods and "n" were used in the HEC-RAS model along with the 12.5m resolution DEM. Then the modelling result was further exported to the RAS Mapper for preparing a floodplain map.

Table 4: Statistical analysis of observed flow depth and flow depth modelled by HEC-RAS

Year	Flow through the weir (m^3/s)	Observed flow depth above weir (m)	Modeled flow depth using different Manning's n																	
			0.025		0.027		0.028		0.030		0.031		0.0315		0.032		0.033		0.035	
a	*b*	*c*	*d*	*c-d*	*e*	*c-e*	*f*	*c-f*	*g*	*c-g*	*h*	*c-h*	*i*	*c-i*	*j*	*c-j*	*k*	*c-k*	*l*	*c-l*
2069	387	2.00	1.7	0.30	1.77	0.23	1.81	-0.11	1.88	0.12	1.92	0.08	1.94	0.06	1.95	0.05	1.99	0.01	2.06	-0.06
2067	289	1.65	1.44	0.21	1.5	0.15	1.53	-0.09	1.59	0.06	1.62	0.03	1.64	0.01	1.65	0.00	1.68	-0.03	1.74	-0.09
2066	251	1.50	1.33	0.17	1.39	0.11	1.42	-0.09	1.47	0.03	1.5	0.00	1.51	-0.01	1.53	-0.03	1.55	-0.05	1.61	-0.11
2072	214	1.35	1.21	0.14	1.27	0.08	1.29	-0.08	1.35	0.00	1.37	-0.02	1.38	-0.03	1.4	-0.05	1.42	-0.07	1.47	-0.12
2070	191	1.25	1.14	0.11	1.19	0.06	1.21	-0.07	1.26	-0.01	1.29	-0.04	1.3	-0.05	1.31	-0.06	1.33	-0.08	1.38	-0.13
Low Flow	116	0.90	0.86	0.04	0.9	0.00	0.92	-0.06	0.96	-0.06	0.97	-0.07	0.98	-0.08	0.99	-0.09	1.01	-0.11	1.04	-0.14
Mean of Flow Depth	Mean & Descripancy	1.44	1.28	11.21%	1.34	7.28%	1.36	5.43%	1.42	1.62%	1.45	-0.23%	1.46	-1.16%	1.47	-2.08%	1.50	-3.82%	1.55	-7.51%
Standard Deviation		0.373	0.285		0.295		0.302		0.311		0.321		0.325		0.325		0.332		0.345	
Co-variance			0.106		0.110		0.113		0.116		0.120		0.121		0.121		0.124		0.129	
Co-relation coeff. R^2			0.999		0.999		0.999		0.999		0.999		0.999		0.999		0.999		0.999	
Nash-Sutcliffe Efficiency				0.516		0.775		0.905		0.953		0.972		0.974		0.967		0.951		0.874

To calculate geometric cross-sections, the DEM layer was placed over the Google Earth satellite image. Further, the satellite image from the Google Earth in conjunction with terrain data from DEM was used as

the base layer for the easy visualization of the river path in RAS Mapper of HEC-RAS. We performed 1D steady flow simulation using HEC-RAS 5.0.5. The basic computational procedure is based on the solution of the one-dimensional energy equation. Energy losses are evaluated by friction (Manning's equation) and contraction/expansion (coefficient multiplied by the change in velocity head). The momentum equation may be used in situations where the water surface profile is rapidly varied [13]. River was defined in RAS Mapper along with riverbank lines and flow paths for each reach as illustrated in Fig. 6. Cross-sections in all reaches were constructed in such a way that they cross the river line in nearly right angle passing through the bank lines and flow paths in respective reaches. This allows the extraction of the cross-section attributes in a systematic way as an input in HEC-RAS for steady flow simulation.

The steady flow was simulated in boundary condition of the normal depth with the input of average bed slope. The simulation result for different flow profile (i.e., corresponding to three return periods) was presented in the map overlaid in Google Earth satellite map for proper visualization of the extent of the flood. An example of defining river line, bank line, flow path and cross-sections in RAS Mapper is presented in Fig. 6 where the terrain map in RAS Mapper was laid over the layer of Web Map Imagery of Google Earth satellite map. The centreline of the river (represented by blue line in Fig. 6) was first defined using zoom feature of the Google Earth satellite image. Similarly, riverbanks (red line in both sides of the blue centre line in Fig. 6) were defined from the same image up to the normal flooding of the river. This gives the width of normal channel of the river. Further, the flow paths (represented by light blue line on both sides of the river in Fig. 6) were defined with the help of same image and terrain map. Cross-section lines of the river were constructed so that they don't intersect each other and cross the river with all defined lines and make right angle to the centre line (i.e., river line). Therefore, the distance between the cross sections is not same. In general, this distance was maintained not to be more than 300m. However, in the case of highly meandered reach, this distance was increased up to 450m to avoid intersection of two cross-sections.

Table 5: Parameterization of variables for HEC-RAS simulation

Reach	Range		Length (m)	Average slope	Catchment area (Sq. Km.)	Flood (m^3/s)			Estimated Manning's roughness coefficient		
						Q_{20}	Q_{50}	Q_{100}	Left over bank	Channel	Right over bank
	Specific Discharge ($m^3/s/Sq.Km.$)					1.9	2.31	2.61			
1	Mardi confluence	Yamdi confluence	6328	0.0164	487.00	925	1125	1271	0.082	0.033	0.082
2	Yamdi confluence	KI Singh bridge	2400	0.0163	534.00	1015	1234	1394	0.082	0.048	0.092
3	KI Singh bridge	Kali Khola confluence	904	0.029	536.00	1018	1238	1399	0.075	0.045	0.075
4	Kali Khola confluence	Phoolbari gorge	1198	0.0058	568.00	1079	1312	1482	0.080	0.048	0.080
5	Phoolbari gorge	Ramghat inlet	1662	0.019	568.00	1079	1312	1482	0.075	0.045	0.075
6	Ramghat inlet	Ramghat outlet	820	0.016	574.00	1091	1326	1498	0.055	0.034	0.050
7	Ramghat outlet	Gharepatan	2347	0.018	574.00	1091	1326	1498	0.075	0.045	0.075
8	Gharepatan	Fushre Khola confluence	4734	0.018	580.00	1102	1340	1514	0.080	0.043	0.080
9	Fushre Khola confluence	Bijayapur Khola confluence	4232	0.0071	753.00	1431	1739	1965	0.062	0.039	0.062
10	Bijayapur Khola confluence	Musetunda	6043	0.013	836.00	1588	1931	2182	0.054	0.034	0.054
11	Musetunda	Kotre confluence	4600	0.0090	848	1611	1959	2213	0.062	0.039	0.062

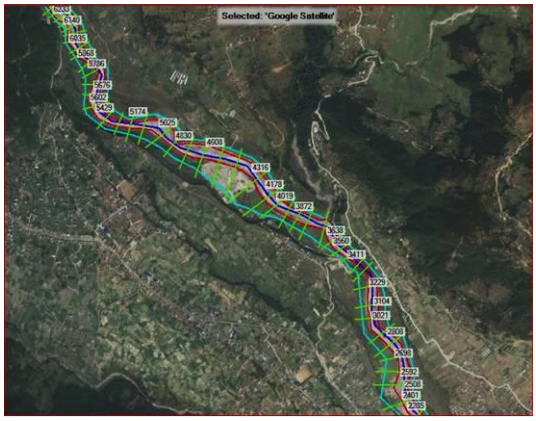

Figure 6: Defining river line, bank line and flow path in RAS Mapper

3.RESULTS AND DISCUSSION

The floodplain map of 20, 50, and 100 years return periods from the RAS Mapper was exported to GIS in raster form for all the 11 reaches. The floodplain map of the study area layered over the DEM is shown in Fig. 7 for 100 years return period. Thus, prepared map was overlaid in the Google Earth map for the better visualization of the flood spread in three different return periods. Using this Google Earth map as the base map, the effect on the settlement was analyzed. Total inundation area along the Seti River for the three return periods in Pokhara Metropolitan City was determined as presented in Fig. 8. The total inundation area was found to be 2.76, 3.05, and 3.59 Km^2 for 20, 50, and 100 years return periods, respectively. The relation of inundation area with respect to return period developed in Fig 8 can be used to predict the flooding area of other return periods in Pokhara City. Fig. 9 shows the maximum depth with respect to flooding associated with the three return periods for the reaches considered for analysis (i.e., except reaches 3, 5 and 7). In general, the depth near the constriction observed to be high because of pooling effect due to insufficient water way of the constriction like gorges, canyon, etc. in the channel course (e.g., reaches 6 and 8).

Figure 7: Floodplain map layered over the DEM

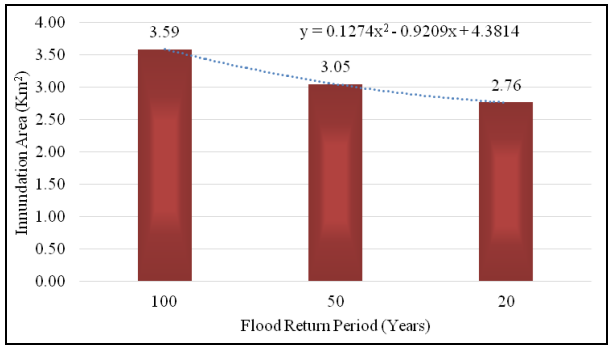

Figure 8: Total inundation area along the Seti River

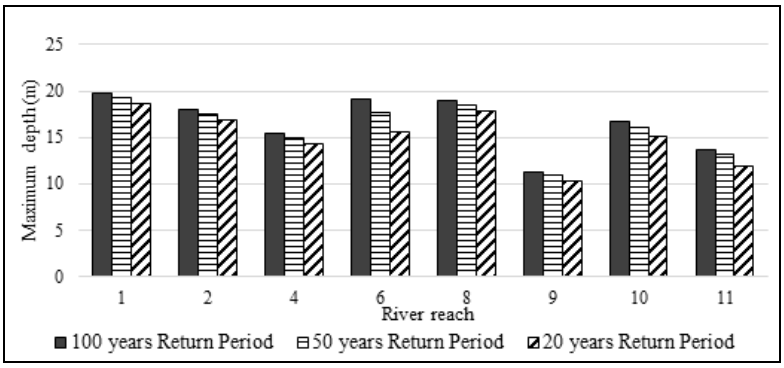

Figure 9: Modelled water depth at the various reaches along the river for the flooding associated with the three different return periods

Floodplain maps prepared from this study for return periods of 20, 50, and 100 years were analysed along various reaches of Seti River in Pokhara. The area covered by the floodplain for 20, 50, and 100 years return period along the reach from Yamdi confluence to KI Singh Bridge is presented in Fig.10.

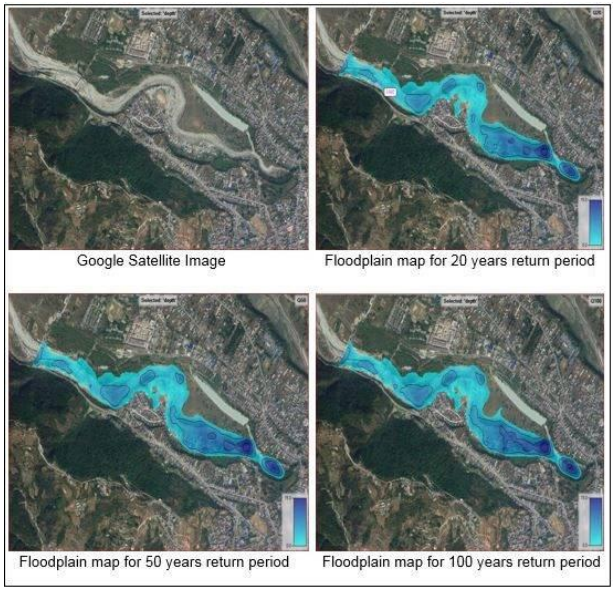

Figure 10: Floodplain map of the Seti River in Yamdi Confluence to KI Singh Bridge for three different return periods (20, 50, and 100 years)

In this reach, the settlement located in Gaighat was found to be at high risk of flood because this area was observed to be flooded with the peak flood of 20 and greater years return period. Same scenario was observed in the reach from Mardi to Yamdi confluence that the settlement situated in Laltin Bazar found to be at high risk as we observed that only the peak flood corresponding to 20 years return period was sufficient to cause flooding in this zone. Similarly, in the reach of Ramghat inlet to Ramghat outlet, the settlement along the bank of the river was found be at risk of flood with peak flood of 50 or larger years return period though this area found to be at lower risk compared to those other areas.

Furthermore, in low land reaches of Fushre Khola confluence to Kotre confluence, with relatively lower bed slope, the agricultural land (without any settlements of infrastructures) was noticed to be at high risk

of the flood as it was found to be inundated with 20 or higher years return period floods. Some photographs of flooding events have been collected and analyzed for the visual comparison of the prepared floodplain map. Previously recorded video of flood in Ramghat and Powerhouse (near the constructing Musetuda-Tiklang Bridge) of actual flooding conditions were compared and found to be matching with the modelled flood plain map. Since the exact date of flooding was not found in video and image records, further analysis was limited to only visual inspection of the flood.

Fig. 11a is the actual flooding condition of the Ramghat in 2016 where the photograph was snapped from a video by the YouTube channel of Junction TV. Fig.11b is the floodplain map for 100 years return period. The arrows in Fig. 11 indicate the flood extent location in real flood (Fig. 11a) and the floodplain map (Fig. 11b). As we visually inspected the extent of flood, the modelled flood extension found to be close to the real flood extension. Fig.12a represents the non-flooding condition of the Musetuda-Tiklang Bridge site. Letters S and T indicate the location of the aggregate stockpile and the tree respectively, which has been the benchmark for comparison of real flood and modelled flood. Fig.12b is the real flooding condition with referenced S and T locations. Fig.12c represents the 20 years floodplain map along with the S and T referenced locations. The referenced locations observed to be comparable between the real flood condition (Fig. 12 b) and floodplain map (Fig. 12c) such that it further supports the reliability of the results obtained from this study that can be used by policy makers, planners, engineers, and insurance agents for various purposes.

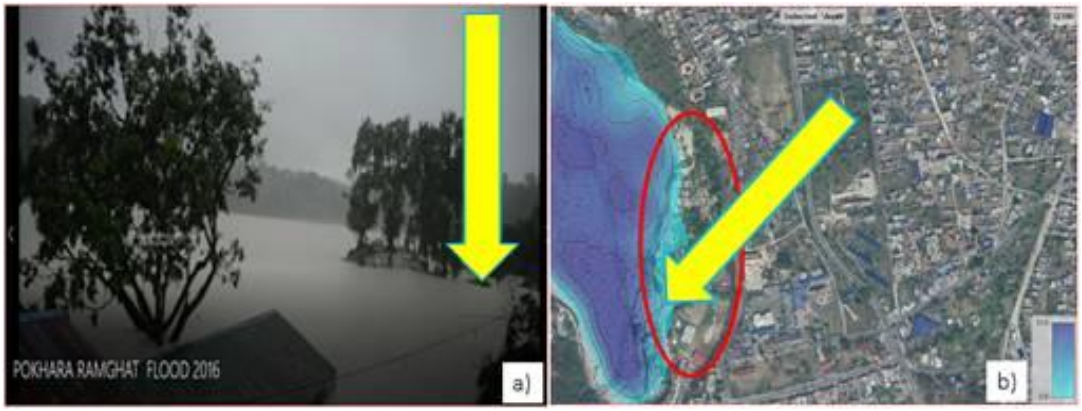

Figure 11: Analysis of a 2016 flood at Ramghat: a) Flooding condition of Ramghat; b) Floodplain map of Ramghat

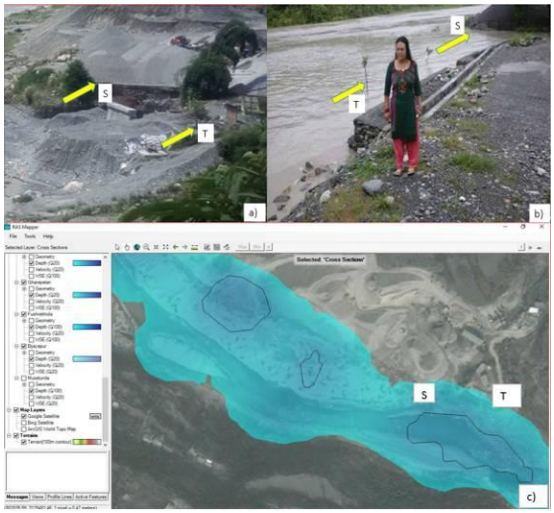

Figure 12 : Flood analysis for the Musetuda-Tiklang Bridge site; a) Site image of non-flood condition; b) Site image of flooding condition; c) Analyzed floodplain map for the site

4. CONCLUSIONS

Annual peak flow of Seti River, which is ungauged, was estimated using catchment area ratio (CAR) method based on annual flow data of 42 years from Mardi gauged station. Flood frequency analysis was performed with thus estimated annual peak flow data of Seti River using Gumbel method for 20, 50, and 100 years return periods. The estimated peak floods found to be comparable (with discrepancy of ≤2.68% only) with the peak floods predicted using Gumbel method based on the annual flow data of Tanahu station (with limited period of data, i.e., 16 years). Therefore, CAR method found to be a reliable strategy to estimate long term annual flow of ungauged river like Seti River.

HEC-RAS model was calibrated first using the estimated value of Manning's roughness coefficient (n) using Cowan approach. Preliminary HEC-AS modelling was performed using surveyed terrain data and flow records over the weir at Tulsighat. As the preliminary simulations result the modelled flow depth close to the measured flow depth tested with the Nash-Sutcliffe efficiency of 0.951, Cowan approach found to be a potential alternative to use for estimating the Manning's roughness coefficient in an ungauged river. So, this approach was utilized to estimate "n" value for various reaches of Seti River. These "n" values can be used as a reference for the future research studies like river flow analysis and scour modelling; and to design hydraulic structures; in the ungauged rivers of Nepal with similar type of slope, riverbed, and meandering conditions.

The estimated roughness was used to model the river flow and the floodplain maps were prepared for 20, 50 and 100 years return periods using available 12.5 m resolution DEM. Floodplain maps prepared from this study were, then, analysed along various reaches of Seti River in Pokhara City. In the reach from Mardi to Yamdi confluence, the settlement in Laltin Bazar and in the reach of Yamdi confluence to KI Singh Bridge, the settlement in Gaighat were observed to be inundated with 20 or greater years return period floods. These areas were found to at high risk of flood compared to the Ramghat area. In the reach of Ramghat inlet to Ramghat outlet, the settlement along the bank of the river was observed to be flooded with peak floods of 50 or larger years return period. However, in low land reaches FushreKhola confluence to Kotre confluence, with relatively lower bed slope, the agricultural land was noticed to be at high risk of the flood as it was found to be inundated with 20 or higher years return period floods. In conclusion, the inundation area along the Seti River in Pokhara City was found to be 2.76, 3.05 and 3.59 Km^2 for a return period of 20, 50, and 100 years, respectively. The methodology developed in this study, including use of Cowan approach to estimate Manning's n, for floodplain mapping of an ungauged river could be beneficial for similar studies in Nepal - where most of the river types are ungauged. As the 12.5 m resolution DEM used for terrain data in HEC-RAS for floodplain mapping is still not sufficient for precise analysis, floodplain maps of this study can be used as the basic floodplain map for general information where the information is scarce. This floodplain mapping is the best alternative for preliminary study and can also be used by the decision makers in the pre-planning of disaster, planning phase of the different infrastructures, projects, programs within the boundary of the floodplain analysis. It is recommended that, during the detailed design of such infrastructures, projects, and programs, precise topographic data should be used. However, the map prepared in this study could be used as a first step by the policy makers and engineers of government authorities like Pokhara Metropolitan City during the formation phase of building by-laws along the Seti River. Further, the insurance engineers of vehicle insurance companies could use the map for estimating the insurance cost of the vehicles located in and near the flood inundated area. The methodology developed in this study is useful for flood analysis study of other ungauged rivers of Nepal. Future modelling efforts could be impactful through investigating river flood for other regions of Nepal and compare the degree of discrepancy on estimated parameters (e.g., peak flood, Manning's n) with the present results. Moreover, future research using the similar modelling approach could consider improvement on the floodplain map by incorporating the DEM with finer resolution (i.e., < 12.5m). As an initiative, we determined total

inundation area that includes water bodies. Future research efforts on this field could improve the utility of the floodplain map by inclusion of classified flood area based on land use, land cover, and flood depth as well.

ACKNOWLWDGEMENTS

Authors would like to acknowledge the Centre of Research for Energy, Environment and Water (CREEW), Kathmandu, Nepal, for providing a research grant to conduct this study.

CONFLICTS OF INTEREST STATEMENT

The authors declare no conflicts of interest for this study.

DATA AVAILABILITY STATEMENT

The data that support the findings of this study are available from the corresponding author upon reasonable request.

REFERENCES

1. G. Rajkarnikar and R. S. Aryal, "Water resources of Nepal in the context of climate change," Kathmandu, 2011.
2. K. Basnet and R. Ettema, "A large-scale particle image velocimetry for resolving unsteady flow features at cylinders," in Proc. 34th World Congress of the International Association for Hydro-Environment Research and Engineering: 33rd Hydrology and Water Resources Symposium and 10th Conference on Hydraulics in Water Engineering, 2011, pp. 3378-3387.
3. National Planning Commission, "15th Plan Approach Paper," Kathmandu, 2019.
4. M. Fort, B. R. Adhikari, and B. Rimal, "Pokhara (Central Nepal): a dramatic yet geomorphologically active environment versus a dynamic, rapidly developing city," Urban Geomorphology, pp. 231-258, 2018.
5. B. Rimal, H. Baral, N. E. Stork, K. Paudyal, and S. Rijal, S., "Growing city and rapid land use transition: assessing multiple hazards and risks in the Pokhara Valley, Nepal," Land, vol. 4, pp. 957-978, 2015.
6. B. Rimal, L. Zhang, H. Keshtkar, X. Sun, and S. Rijal, "Quantifying the spatiotemporal pattern of urban expansion and hazard and risk area identification in the Kaski district of Nepal," Land, vol. 7, no. 1, 2018.
7. J. Goodhand, O. Walton, J. Rai, and S. Karn, "Marginal gains: borderland dynamics, political settlements, and shifting centre-periphery relations in post-war Nepal," Contemporary South Asia, vol. 29, no. 3, pp. 311-329, 2021.
8. J. Kargel, G. Leonard, L. Paudel, D. Regmi, S. Bajracharya, and M. Fort, "The 2012 Seti River flood disaster and alpine cryospheric hazards facing Pokhara, Nepal," Geophysical Research Abstracts, EGU General Assembly, vol. 16, no. 1, 2014.
9. A. Bordbar, M. Heidarnejad, A. Gholami, and S. Lacks, "Calibration of Manning's roughness coefficient in the rivers," Int. Journal of Agriculture & Crop Science, vol. 4, no. 21, pp. 1562-1564, 2012.
10. W. Marquardt, "Trends in computer-aided process modelling," Computers & Chemical Engineering, vol. 20, pp. 591-609, 2003.
11. P. V. Timbadiya, P. L. Patel, and P. D. Porey, "Calibration of HEC-RAS model on prediction of flood for lower Tapi River, India," Journal of Water Resource & Protection, vol. 3, no. 11, pp. 805-811, 2011.
12. V. T. G. Boulomytis, A. C. Zuffo, J. G. Dalfré Filho, and M. A. Imteaz, "Estimation and calibration of Manning's roughness coefficients for ungauged watersheds on coastal floodplains," Int. Journal of River Basin Management, vol. 15, no. 2, pp. 199-206, 2017.
13. HEC. (2023). Hydrologic Engineering Center, US Army Corps of Engineers. [Online]. Available: https://www.hec.usace.army.mil/software/hec-ras/.

14. M. S. Horritt and P. D. Bates, "Evaluation of 1D and 2D numerical models for predicting river flood inundation," Journal of Hydrology, vol. 268, pp. 87-99, 2002.

15. M. R. Dhital, R. Shrestha, G. B. Shrestha, and D. Tripathi, "Hydrological hazard mapping in Rupandehi district, West Nepal," Journal of Nepal Geological Society, vol. 31, pp. 59-66, 2007.

16. E. Abazi, "Calibration of hydraulic model for Buna River," Journal of Int. Environmental Application & Science, vol. 11, no. 2, pp. 198-206, 2016.

17. M. S. Khattak, F. Anwar, T. U. Saeed, M. Sharif, K. Sheraz, and A. Ahmed, "Floodplain mapping using HEC-RAS and ArcGIS: a case study of Kabul River," Arabian Journal for Science & Engineering, vol. 41, no. 4, pp. 1375-1390, 2016.

18. A. Shrestha, S. Thapa, and B. N. Ghimire, "Flood hazard mapping and vulnerability analysis along Seti River in Pokhara Metropolitan City," Lecture Notes in Civil Engineering, vol. 115, 2021. Available: http://www.springer.com/series/15087.

19. B. Gauchan, "Flood risk mapping for East Rapti River, Nepal using GIS and HEC-RAS," M.S. thesis, Indian Institute of Technology, Roorkee, 2005.

20. D. K. Gautam and R. G. Kharbuja, "Flood plain mapping using GIS informatic tools," Journal of Hydrology & Meteorology, vol. 3, no. 1, pp. 1-8, 2006.

21. S. Dangol and A. Bormudoi, "Flood hazard mapping and vulnerability analysis of Bishnumati River, Nepal," Nepalese Journal on Geoinformatics, vol. 14, pp. 20-24, 2015.

22. P. Banstola and B. Sapkota, "Flood risk mapping and analysis using hydrodynamic model HEC-RAS: a case study of Daraudi River, Chhepatar, Gorkha, Nepal," Grassroots Journal of Natural Resources, vol. 2, no. 3, 2019.

23. J. Kim, C. Lee, W. Kim, and Y. Kim, "Roughness coefficient and its uncertainty in gravel-bed river," Water Science & Engineering, vol. 3, no. 2, pp. 217-232, 2010.

24. K. Basnet and D. Acharya, "Flood analysis at Ramghat, Pokhara, Nepal using HEC-RAS," Technical Journal, vol. 1, pp. 41-53, 2019.

25. R. Karki, R. Talchabhadel, J. Aalto, and S. K. Baidya, "New climatic classification of Nepal," Theoretical & Applied Climatology, vol. 125, pp. 799-808, 2016.

26. K. Basnet, U. Baniya, and S. Karki, "Comparative study of design discharge calculation approaches, a case study of Padhu Khola, Kaski, Nepal," Oodbodhan, vol. 5, no. 5, pp. 15-18, 2018.

27. K. Subramanya, "Engineering Hydrology," 3rd ed. Kanpur, India: McGraw-Hill, 2008.

28. C. C. Gianfagna, C. E. Johnson, D. G. Chandler, and C. Hofmann, "Watershed area ratio accurately predicts daily streamflow in nested catchments in the Catskills, New York," Journal of Hydrology: Regional Studies, vol. 4, pp. 583-594, 2015.

29. A. Elona, "Calibration of hydraulic model for Buna River," Journal of Int. Environmental Application & Science, vol. 11, no. 2, pp. 198-206, 2016.

30. W. L. Cowan, "Estimating hydraulic roughness coefficients," Agricultural Engineering, vol. 37, no. 7, pp. 473-475, 1956.

31. A. W. Marcus, K. Roberts, L. Harvey, and G. Tackman, "An evaluation of methods for estimating Manning's n in small mountain streams," Mountain Research & Development, vol. 12, no. 3, pp. 227-239, 1992.

32. N. Nut, "Floodplain mapping using HEC-RAS and GIS in Nam Phong River Basin, Thailand," Int. Journal of Environmental & Rural Development, vol. 6, no. 1, pp. 153-158, 2015.

33. W. Zhang and D. R. Montgomery, "Digital elevation model grid size, landscape representation," Water Resources Research, vol. 30, no. 4, pp. 1019-1028, 1994.

APPENDIX

Table A1. Cowan's component method of estimating Manning's n taken from [31].

Component	Channel morphology and condition	Value
n_0	Sediment type	
	Earth	0.02
	Rock cut	0.025
	Fine Gravel	0.024
	Coarse Gravel	0.028
n_1	Degree of irregularity (e.g., jagged channel cross section)	
	Smooth	0
	Minor	0.005
	Moderate	0.001
	Severe	0.02
n_2	Variations in channel cross-sectional shape and area (e.g., shifting of main flow from side to side)	
	Gradual	0
	Alternating occasionally	0.005
	Alternating frequently	0.010-0.015
n_3	Relative effect of obstructions (e.g., logs, piling, boulders etc)	
	Negligible	0
	Minor	0.010-0.015
	Appreciable	0.020-0.050
	Severe	0.040-0.060
n_4	Vegetation	
	Low	0.005-0.010
	Medium	0.010-0.025
	High	0.025-0.050
	Very high	0.050-0.100
m_5	Degree of meandering	
	Minor, sinuosity = 1.0-1.2	1
	Appreciable, sinuosity = 1.2-1.5	1.15
	Severe, sinuosity > 1.5	1.3